Drainage and reinforcement effect of steel drainage pipes in stabilization of levee subjected to seepage flow

J. Singh, K. Horikoshi & A. Takahashi
Department of Civil and Environmental Engineering, Tokyo Institute of Technology, Japan

ABSTRACT: The structure such as levee tends to remain stable on the account of the additional strength contributed by the matric suction when the soil is in an unsaturated condition. Flooding in the river channel causes seepage flow and rise in phreatic surface in the levee resulting major portion of the levee to be in saturated condition. The decrease in the zone of unsaturated soil in the levee, in absence of the proper protection at the toe region of the slope on protected side, can cause failure of slope and sometimes even cause breaching of the levee. In this study, the installation of the steel pipes having the spiral blades and holes on the surface is proposed to use for stabilization of levees subjected to seepage flow. Series of geotechnical centrifuge tests were conducted to understand the roles of the steel drainage pipes as drainage and reinforcement against sliding. The centrifuge tests result shows that with the installation of the steel drainage pipes, the phreatic surface in the levee during the flooding is lowered and drainage of water is enhanced compared to the unreinforced case. This lowering of the phreatic surface prevents the loss of the strength of soil by keeping the soil in an unsaturated condition. The installation of pipes also restrict the deformation of the slope through mobilization of axial force thus increasing the overall resistance of the levee against the flood-induced deformation.

1 INTRODUCTION

River levees are geotechnical structures providing the barrier for the area near a river from river-induced disasters. River levees are subjected to increased seepage flow when there is flooding in the river channel. Increased seepage flow in levees can cause destabilization by reduction of shear strength due to the conversion of soil from unsaturated to saturated (Hori et al. 2011; Vandamme and Zou 2013).

Many researchers through their study have shown the vulnerabilities of slope when subjected to seepage flow. Study through centrifuge experiments on the slope showed the triggering of slope failure is caused by loss of shear strength and the expansion of saturated zone when subjected to seepage flow (Timpong et al. 2007). Oya et al. (2015) through their field study and numerical analysis of Saigon River showed that the existence of higher phreatic surface within river bank has the negative influence on the stability.

From all these studies, the need for the protection in the slope subjected to the seepage flow is made obvious. As per the previous study, the protection can be provided through drainage which can cause limitation in the rise in the pore water pressure by lowering the phreatic surface of the slope. Also, protection can be provided through reinforcement which provides the additional strength to compensate the loss of the shear strength in the levee subjected to seepage flow to provide stability to slopes.

Traditionally, protection measures used in levees against seepage flow can provide either drainage or reinforcement function. Drainage pipes ensure the significant portion of the levee remains in unsaturated condition (Rahardjo et al. 2003, 2011). However, drainage pipes also have some limitations such as its performance of draining the water being affected by the hydraulic properties of the soil and inability to increase the performance in slope stability beyond the critical length of drainage (Cai et al. 1998; Chen and Chen 2016). Drainage pipes also have the limited zone of the influence in slope regarding stability performance (Ghiassian and Ghareh 2008).

Soil nails predominantly with the development of axial force increase the shear resistance in the slope (Cai and Ugai 2003). Ng et al. (2006) and Rotte and Viswanadham (2012) through the series of the centrifuge experiments and Zhou et al. (2009) from full-scale test confirmed the effectiveness of soil nail in the global stability of the slope subjected to seepage flow. However, in these studies, limitation of soil nail performance was also shown, as soil nails were capable of only delaying and minimizing the formation of the crack and local failure but not prevent it. The levee protection measures with only either of drainage or reinforcement showed its limitation in slope

protection when subjected to seepage flow. In this study, therefore, the possibility of use of the steel drainage pipe in the levee for the protection against seepage-induced failure is investigated through the series of the centrifuge experiments. Steel drainage pipes are the tubular steel pipes with numerous holes on the surface and are provided with the spiral blades at the end, therefore, capable of providing both drainage and reinforcement.

2 CENTRIFUGE EXPERIMENT

2.1 *Test setup and arrangement of instruments*

Three different cases of levees subjected to seepage flow with varying degree of the protection are presented in the paper. The test setup and arrangement of sensors are described in this section in prototype scale unless otherwise mentioned. Figure 1 shows the geometry of model slope and arrangement of pipes in the centrifuge models (Cases 1-3). The model consists of the 2 m thick foundation layer and 4 m high embankment with the 1H: 1V slope. The total width of the model ground is 12 m, and the length of the model is 3 m. The setup is also provided with the upstream water supply reservoir and downstream drainage reservoir each of 1 m width. The boundary between the upstream reservoir and soil model is made of the mesh-like steel wall, and that of drainage reservoir and soil model is made by a solid steel wall. During the process of the making ground, miniature pore water pressure transducer (PPT) sensors with wire mesh head [Model: SSK Micro Pressure Transducer P306V-02] are also placed in a predetermined location (location A, B, C and D in Fig. 1) with precise measurement. Figure 1 (a) shows the cross-section of the model for all the cases. In Cases 2 and 3, the pipes are installed at 1m height from the ground surface. Figure 1 (b) shows the arrangement of the pipes in the plan view for the Cases 2 and 3. In these cases, the slope is provided with three pipes. The pipes are installed at the spacing of the 1 m. In all the cases, the surface layer of 0.2 m made of soil mixed with the fiber is provided on the slope. The surface layer of the soil and fiber mixture models the grass cover, common in such structures. Two laser displacement transducers (LDT) are used to measure the settlement at shoulder end and on the slope surface above the location of PPT 'A'. Both the LDTs has the sensor head of LB-02 series manufactured by Keyence. However, the amplifiers used are two types of LB60 and LB62 series with the measurement range of ±40 mm and ±10 mm respectively. Marked noodles are placed on the side face of the model for visual observation of the deformation pattern through the transparent window. The test conditions are summarized in Table 1. These cases allowed to study the effectiveness of the steel drainage pipes in slope stabilization and also to understand the contribution of drainage function and reinforcement function.

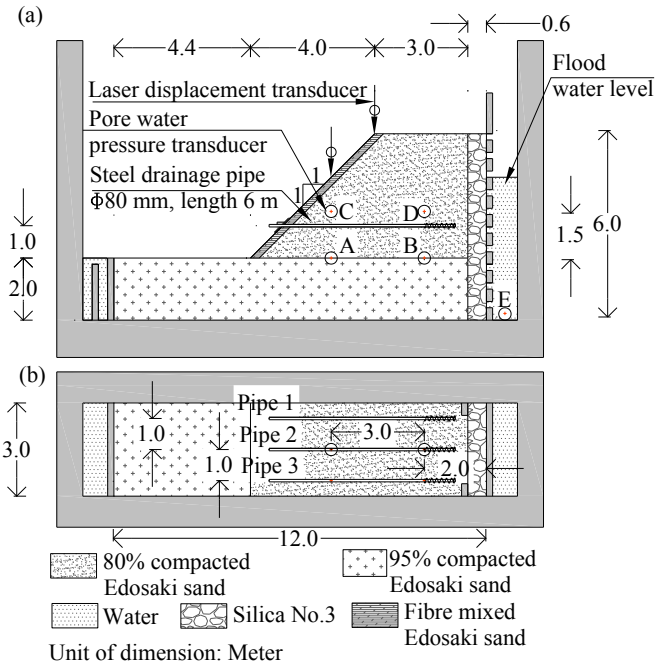

Figure 1. Model Configuration (a) sectional view with geometry and location of sensors (b) plan view for Cases 2-3

Table 1. Protection conditions in models

Cases	Level of protection	Description of protection					
		Pipe 1		Pipe 2		Pipe 3	
		R	D	R	D	R	D
Case 1	Unreinforced	n/a	n/a	n/a	n/a	n/a	n/a
Case 2	Reinforced (3 steel drainage pipes)	○	○	○	○	○	○
Case 3	Reinforced (3 steel drainage pipes)	○	○	○[a]	×	○	○

Note: R= reinforcement function, here pipe made of steel; D= drainage function, here pipes is tubular with holes on the surface; n/a= not available, pipes not used; a= with sensors to measure axial force and bending moment.

2.2 *Material Properties*

Edosaki sand is used in the preparation of the model. The properties of Edosaki sand are shown in Table 2. The material is classified as silty sand (SM) according to USCS. Foundation and embankment are compacted at 95% (1.72 g/cm^3) and 80% (1.45 g/cm^3) of dry density, respectively. The soil water characteristic curve (SWCC) for the embankment along with the parameters for van Genuchten model is shown in Fig. 2. The SWCC presented here is wetting type obtained by the column test. The SWCC is measured by allowing water to be drawn up in soil from water supplied at the base of soil column (Fredlund et al. 2012). The surface layer on the slope is prepared by soil mixed

with fiber to replicate the grass cover often found in the real levee and to prevent the occurrence of unrealistic surface erosion during the experiment. The content of the fiber is 1% of the dry weight of sand.

Table 2. Properties of the Edosaki sand

Soil properties	Values
D50 (mm)	0.30
D10 (mm)	0.01
Coefficient of uniformity	38.00
Coefficient of gradation	8.53
Soil particle density (g/cm^3)	2.72
Optimum moisture content	14.5%
Average initial water content of model ground	14.7%
Angle of shearing resistance (degrees)	
embankment soil without fiber	29
embankment soil with 1% fiber	31
Cohesion (kN/m^2)	
embankment soil without fiber	2.5
embankment soil with 1% fiber	4.2
Saturated coefficient of permeability (m/s)	
Foundation	1.5E-6
Embankment	4.5E-5
Dry density for embankment (g/cm^3)	1.45
Dry density of foundation (g/cm^3)	1.72

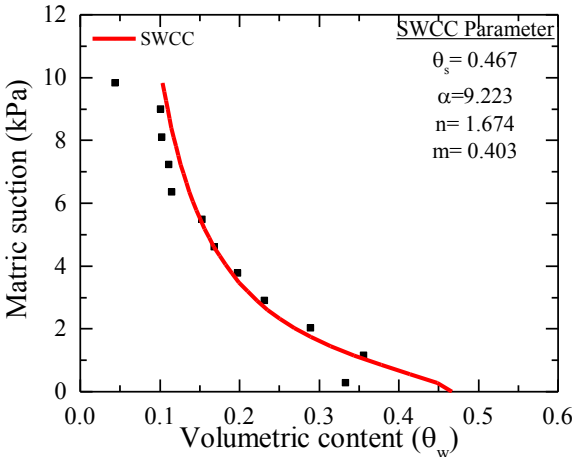

Figure 2. Soil water characteristic curve (SWCC) for embankment soil

The polyester fibers named Teijin RA04FN, approximately 39 μm in diameter and 5 mm in length was used in the test. Steel drainage pipes are used as protection in levee against seepage induced deformation for different cases of the test. Steel drainage pipes, which are tubular steel pipes are provided with holes of the diameter 24 mm at the spacing of 0.16 m on the surface. The end one-meter length of the pipe is provided with the spiral blade of the external diameter 0.16 m. These pipes provide both drainage and reinforcement functions. The one tubular steel pipe (Pipe 2) with the same configuration and made of the same material but filled with glue is used in Case 3 to measure the axial force and bending moment with the help of strain gauges attached to the surface. Properties of the steel drainage pipes used in the experiment in the prototype scale are summarized in Table 3.

Table 3. Properties of steel drainage pipe

Parameters	Values
Internal diameter (mm)	60
External diameter (mm)	80
Length (m)	6
Pitch of the screw (mm)	160
Thickness of plate forming screw (mm)	20
External diameter of screw part (mm)	160
Young's Modulus, E (N/m^2)	2.10E+11
Poisson's ratio, v	0.3

2.3 *Testing Procedure*

After all the set-up has been completed, saturation of foundation layer is carried out. For all the cases, the water level at the top of the foundation level is considered as the initial state. For saturation, de-aired water is supplied to the water supply reservoir until the volume of the water supplied to the foundation layer exceeded the calculated volume of the pores. After the completion of saturation of the foundation at 1g, centrifugal acceleration is increased in steps to the target 20g. After the centrifugal acceleration has reached to 20g, steady state is ensured by allowing the pore water pressure measurement to become stable. The phenomenon of the flood in the river channel is then simulated in the centrifuge experiment by raising the water level in the water supply reservoir. Figure 3 shows the time history of flood water head supplied in the supply reservoir. Rising rate of the flood water is in a range of 0.03-0.06 m/hr.

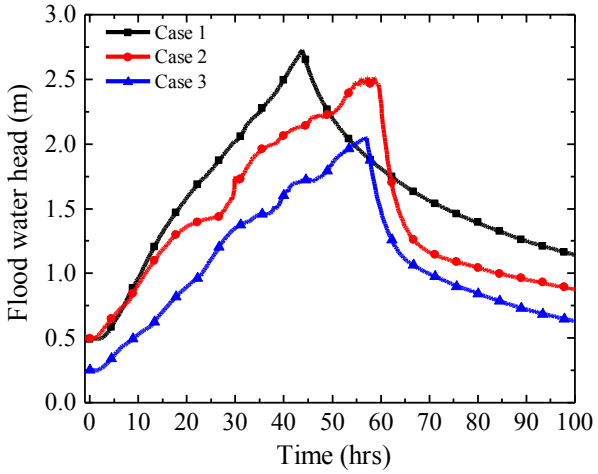

Figure 3. Time histories of supply flood water head.

3 RESULTS AND DISCUSSION

The effectiveness of the steel drainage pipe on limiting the propagation of failure surface is investigated by comparison of reinforced cases (Cases 2 and 3) with the unreinforced case (Case 1). Deformation of the levee is evaluated through the observations of marked noodles through transparent window and measured displacement using the LDTs. Figure 4 shows the superimposed images of the levee at initial

condition and after the seepage test for all the cases along with initial shape, deformed shape, and slip line. In Case 1, the slip line extends from the toe to the crest of the levee as shown in Fig. 4 (a). In this case, the failure starts from the toe region and progressively extends to the crest causing the complete collapse of the levee. Thus, the retrogressive failure mode is observed. In Case 2, with the presence of the steel drainage pipes, seepage-induced failure is prevented as shown in Fig. 4 (b). In Case 3, even though levee suffered erosion below the location of the pipe before the seepage test (while increasing centrifugal acceleration), the collapse of the levee is prevented. In this case, the continuation of the slip line is stopped beyond the location of the pipes. The presence of erosion below the toe region before seepage test facilitated the continuation of erosion, especially above the pipes during the rise of the flood water. Along with this, tension cracks are observed on the crest of the levee. However, significant movement of the soil mass is prevented as shown in Fig. 4 (c).

Figure 5 shows the time histories of settlement at the surface of the slope above location A, along with the indication of the initiation of the movement represented by the vertical line for Cases 1 and 3. In Case 1, failure is initiated after 22 hrs of seepage flow and at the flood head of 1.67 m. In Case 3, the presence of soil erosion before seepage flow initiated significant slide after 50 hrs of seepage flow when the flood head reaches around 1.84 m. However, in Case 3, the settlement is restricted, and the total collapse of the slope is prevented.

3.1 *Drainage contribution*

The drainage of the seepage water from the river levee is improved with the use of the steel drainage pipes and thus limiting the rise in the pore water pressure in the slope. Figure 6 shows the variation of the discharge rate with the flood water head for different cases. The discharge rate here is calculated from the change in the level of water in drainage tank measured from PPT installed in it. The discharge rate is much larger in the case where the levee is protected by steel drainage pipes (Cases 2 and 3) compared to the unreinforced case (Case 1). In the case with the drainage, sharp rise of the discharge rate is observed when the flood head exceeds 1.5 m. Since the pipes are installed at 1 m height from the ground surface, the effectiveness of pipe to drain the water is observed when flood head is above it as shown in the Fig. 6. The levee without steel drainage pipe has significantly low discharge rate. Figure 7 shows the changes in the pore water pressure at the locations A and B with the flood water head for three cases. The improved drainage due to the pipes cause the lowering of the phreatic surface especially near the slope as indicated by the restricted rise in pore water pressure at location A. The effectiveness of lowering phreatic surface decreases along the length of the pipe as shown by limited difference in the pore water pressure at location B among the cases**.** Nonetheless, the drainage pipe is effective in restricting pore water pressure buildup near the slope toe, hence allows the soil to remain in an unsaturated condition which is crucial for slope stability.

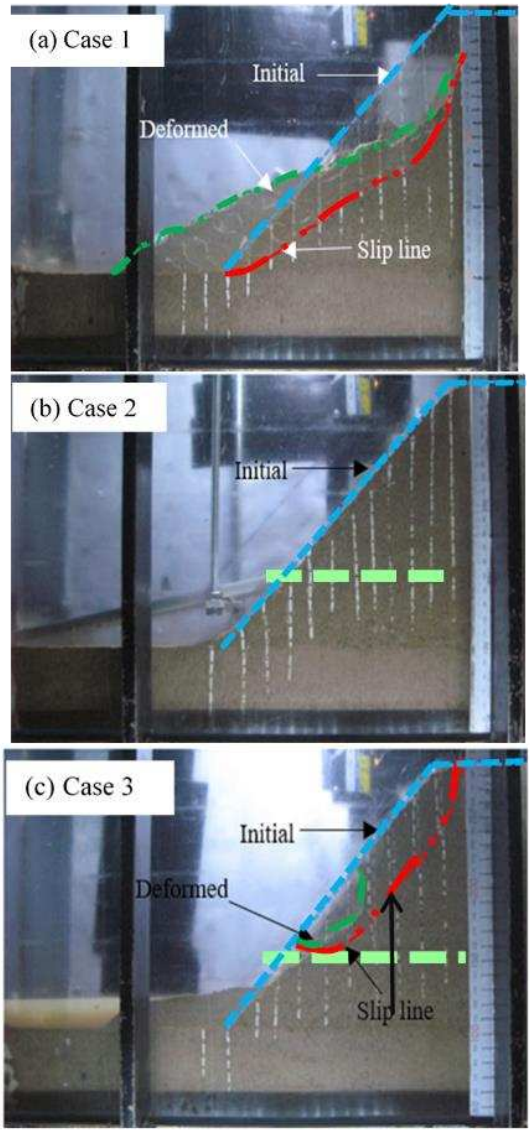

Figure 4. Superimposed image of initial condition with deformed shape (a) Case 1; (b) Case 2; (c) Case 3

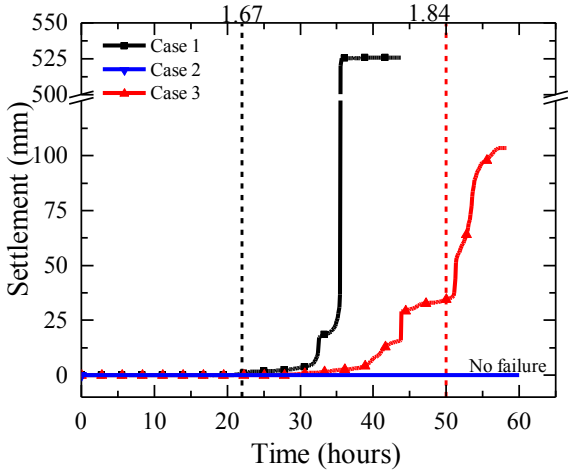

Figure 5. Time histories of settlement on slope above location A

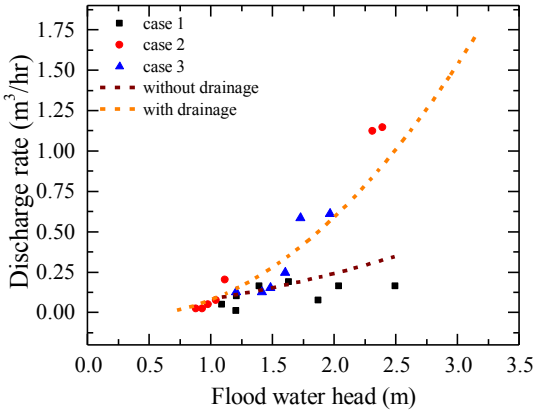

Figure 6. Change in discharge rate with flood water head

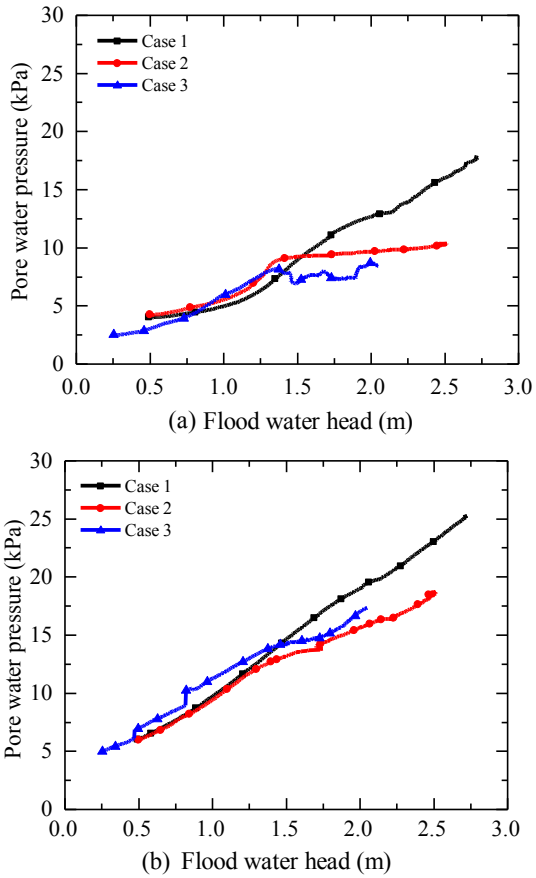

Figure 7. Development of pore water pressure with flood water head (a) at location A; (b) at location B.

3.2 *Reinforcement contribution*

For understanding the contribution of the reinforcement of the purposed steel drainage pipe against the seepage-induced failure, the strain gauges to measure the axial forces and bending moment are installed in the central pipe in Case 3. Figure 8 shows the time history of the axial force near the facing plate (at 0.4 m from the slope surface) and the supply flood head for Case 3 respectively. The axial force is set the zero at the beginning of the seepage test. The axial force further can be decomposed to the end reaction contributed by the spiral blades at the end of the pipe and the skin friction between the soil and section of pipe without spiral blade as shown in Fig. 8 (a**).** The axial force is mobilized with the rise of the flood water head once the flood water head exceeds 1.5 m as shown in the Fig. 8.

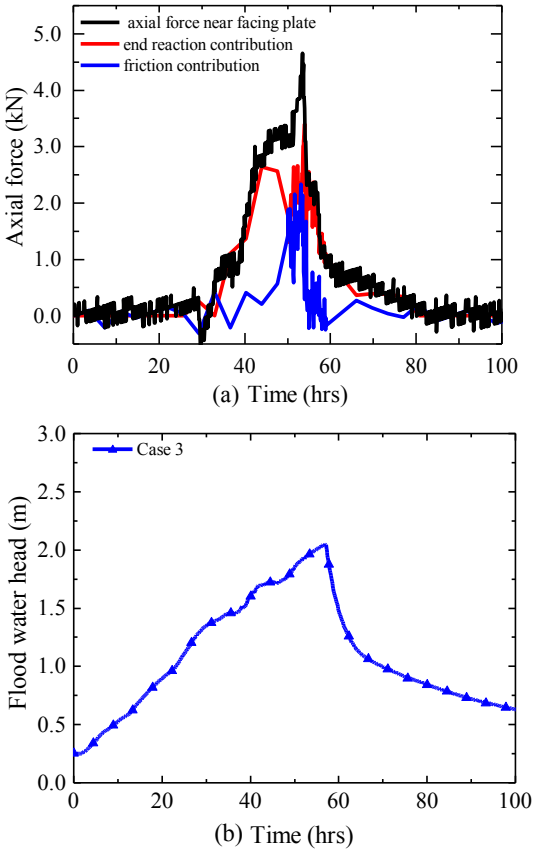

Figure 8. Time histories of (a) axial force near facing plate with components (b) water supply head in Case 3

The axial force is predominantly mobilized through the end reaction initially, and with the rise of the flood water head and possibly due to induced deformation, skin friction also contributes to axial force mobilization. This mobilized axial force provides additional confinement to the soil in the shallower portion of the slope and contributes to the stability of the slope by compensating the strength reduction caused by saturation of the soil. Bending moment at the different distance from slope surface along the length of the pipe at the different relevant times are plotted along with the soil reaction on the pipe is shown for Case 3 in Fig. 9. The bending moment is measured by the strain gauges placed at four different locations on the pipe surface. The embedment length of the pipe is 5.6 m, and distance of 0 m from the slope surface correspond to 0.4 m from the tip of the pipe. The section with the spiral blades is from 4.6 m to 5.6 m from the slope surface. Bending moment is analyzed by setting the bending moment equal to zero at the start of seepage flow. Soil reaction is obtained by double differentiation of bending moment using the weighted residual numerical differentiation as described in Brandenberg et al. (2010). The soil reaction calculated is minimal compared to the static load induced on the pipe by weight of slope. This suggests

that the reinforcement contribution is, therefore, predominantly through the mobilization of the axial force and minimally through the bending moment.

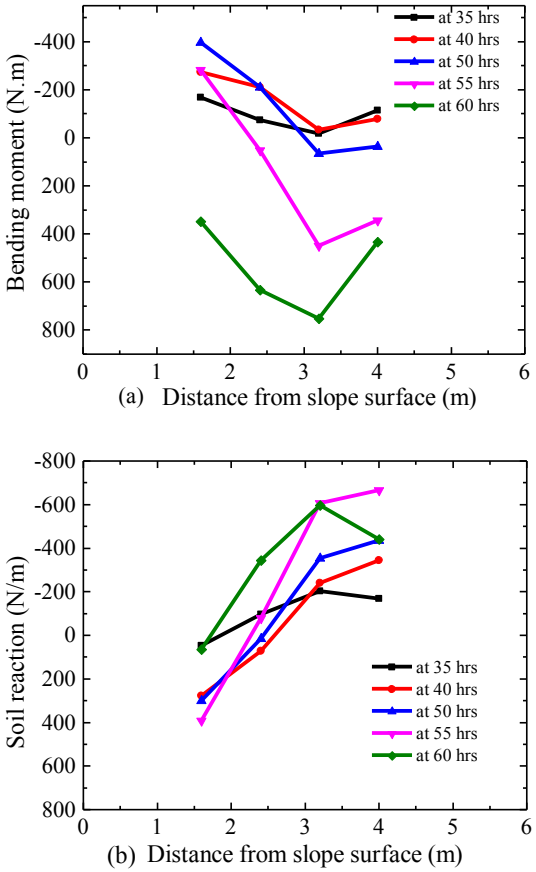

Figure 9 (a) Bending moment (b) earth reaction along length of pipe in Case 3

4 CONCLUSION

The effectiveness of the steel drainage pipe which can protect levee both by drainage and reinforcement against the flood-induced deformation in the levee is demonstrated in this paper by the centrifuge model tests. In the paper, one case of the unreinforced slope and additional two cases of levee protected by steel drainage pipes are presented. The contribution of each function of the proposed steel drainage pipes in the slope protection is also investigated. Experiment results reveal that installation of the steel drainage pipes (i) allows the levee to withstand the higher flood water head and the longer flood duration and (ii) is effective to limit the continuation of slip line in the slope. This resistance against the flood induced deformation is achieved through the combined function of drainage and reinforcement provided by steel drainage pipe. Improved drainage of seepage water allowed lowering of phreatic surface and hence more soil to remain in unsaturated condition. Reinforcement through mobilisation of axial force also contributed to overall resistance against flood induced deformation by providing additional confinement to the soil in shallower portion.

5 REFERENCES

Brandenberg, S.J., Wilson, D.W. & Rashid, M.M. 2010. Weighted Residual Numerical Differentiation Algorithm Applied to Experimental Bending Moment Data. *Journal of Geotechnical and Geoenvironmental Engineering* 136(6): 854–863.

Cai, F. & Ugai, K. 2003. Reinforcing mechanism of anchors in slopes: a numerical comparison of results of LEM and FEM. *International Journal for Numerical and Analytical Methods* 27: 549–564.

Cai, F., Ugai, K., Wakai, A. & Li, Q. 1998. Effects of horizontal drains on slope stability under rainfall by three-dimensional finite element analysis. *Computers and Geotechnics* 23: 255–275.

Chen, C.N. & Chen, H.Y. 2016. Distributions of Pore Water Pressure Surround a Horizontal Drain Pipe on a Retaining Wall Under Steady State Condition. *Journal of Mechanics* 29(2): 263–272.

Fredlund, D.G., Rahardjo, H. & Fredlund, M.D. 2012. *Unsaturated soil mechanics in engineering practice*. John Wiley & Sons.

Ghiassian, H. & Ghareh, S. 2008. Stability of Sandy Slopes Under Seepage Conditions. *Landslides* 5(4): 397–406.

Hori, T., Mohri, Y., Kohgo, Y. & Matsushima, K. 2011. Model Test and Consolidation Analysis of Failure of a Loose Sandy Embankment Dam during Seepage. *Soils and foundations* 51(1): 53–66.

Ng, C.W.W., Zhang, L.M. & Wang, Y.H. 2006. The effects of soil nails in a dense steep slope subjected to rising groundwater. *Proceedings of Physical modelling in geotechnics : 6th ICPMG '06:* 397–401.

Oya, A., Bui, H.H., Hiraoka, N., Fujimoto, M. & Fukagawa, R. 2015. Seepage flow-stability analysis of the riverbank of Saigon river due to river water level fluctuation. *International Journal of GEOMATE*, 8(15): 1212-1217

Rahardjo, H., Hritzuk, K.J., Leong, E.C. & Rezaur, R.B. 2003. Effectiveness of horizontal drains for slope stability. *Engineering Geology* 69: 295–308.

Rahardjo, H., Santoso, V.A., Leong, E.C., Ng, Y.S. & Hua, C.J. 2011. Performance of Horizontal Drains in Residual Soil Slopes. *Soils and Foundations* 51(3): 437–447.

Rotte, V.M. & Viswanadham, B.V.S. 2012. Performance of 2V:1H Slopes with and without Soil-Nails Subjected to Seepage: Centrifuge Study. *Proceeding of GeoCongress, ASCE:* 643–652.

Timpong, S., Itoh, K. & Toyosawa, Y. 2007. Geotechnical centrifuge modelling of slope failure induced by ground water table change. *Proceeding of Landslide and Climate change*: 107–112.

Vandamme, J. & Zou, Q. 2013. Investigation of slope instability induced by seepage and erosion by a particle method. *Computers and Geotechnics* 48: 9–20.

Zhou, Y.D., Cheuk, C.Y. and Tham, L.G. 2009. Numerical modelling of soil nails in loose fill slope under surcharge loading. *Computers and Geotechnics* 36: 837–850.